ISSN 0869-5911, Petrology, 2016, Vol. 24, No. 4, pp. 315–335. © Pleiades Publishing, Ltd., 2016.
Original Russian Text © V.A. Lebedev, O.Z. Dudauri, M.G. Togonidze, Yu.V. Gol'tsman, 2016, published in Petrologiya, 2016, Vol. 24, No. 4, pp. 339–362.

The Age of Young Intrusions of Tsana Complex (Greater Caucasus) and Isotope-Geochemical Evidence for Their Origin from Hybrid Magmas

V. A. Lebedev[a], O. Z. Dudauri[b †], M. G. Togonidze[b], and Yu. V. Gol'tsman[a]

[a] *Institute of Geology of Ore Deposits, Petrography, Mineralogy, and Geochemistry, Russian Academy of Sciences, Staromonetny per. 35, Moscow, 119017 Russia*

e-mail: leb@igem.ru

[b] *A. Janelidze Institute of Geology, I. Javakhishvili Tbilisi State University, A. Politkovskaya st., 5, Georgia, Tbilisi, 0186*

Received December 7, 2015; in final form, January 20, 2016

Abstract—This paper presents isotope-geochronological and petrological study of granitoids of the potentially ore-bearing (Au–As–Sb–Sn–Mo) Early Pliocene Tsana Complex, which are confined to the Main Caucasus fault zone (upthrow fault) in the central part of the Greater Caucasus Range. The Tsurungal and Karobi groups of magmatic bodies are distinguished based on spatial criterion. The Tsurungal group includes three small granite—granodiorite massifs (Tsurungal, Chorokhi, and Toteldash) and numerous acid and intermediate dikes in the upper reaches of the Tskhenistsqali River (Kvemo Svaneti, Georgia). The Karobi group comprises three subvolcanic rhyodacite bodies located in the upper reaches of the Chashuri River (Zemo Racha, Georgia) and numerous N–S-trending trachyandesite dikes near the axial zone of the Main Caucasus Range. The K-Ar and Rb-Sr isotope dating shows that the granitoid massifs and dike bodies of the Tsana Complex were formed in two different-age pulses of the Pliocene magmatism: phase I at 4.80 ± 0.15 and phase II at 4.15 ± 0.10 Ma. All hypabyssal rocks of the Karobi group, unlike those of the Tsurungal Group, were formed during the first pulse. Petrographic studies in combination with geochemical data indicate that most of the granitoids of the Tsana Complex are hybrid rocks (I-type post-collisional granites) and were derived through mixing of deep-seated mantle magmas with acid melts obtained by the upper crustal anatectic melting in the Main Caucasus fault zone. The granitoids of the Tsurungal Group define basic to acid evolution (diorite–granodiorite–granite–two-mica granite) possibly caused by both crystallization differentiation and increasing role of crustal contamination in the petrogenesis of the parental magmas of these rocks. This conclusion is also confirmed by the differences in the Sr isotope composition between granitoids of the early ($^{87}Sr/^{86}Sr = 0.7053$) and late ($^{87}Sr/^{86}Sr = 0.7071$) phases of the Tsana Complex. Main trends in spatiotemporal migration of magmatic activity in the central part of the Greater Caucasus in the Pliocene–Quaternary time were established using obtained and earlier published isotope-geochronological data.

DOI: 10.1134/S0869591116040032

INTRODUCTION

A vast neovolcanic province has been formed during last 8.5–8 Ma up to the Late Pleistocene–Holocene at the territory of the Greater Caucasus and its foothills, which bound the Eurasian–Arabian continental collision zone to the north (Chernyshev et al., 2006). The intense volcanic activity manifested by ejections of several large stratovolcanoes (Chegem, Elbrus, Kazbek, and Kabardzhin) and numerous monogenic volcanic vents (Lebedev and Vashakidze, 2014 etc.) in this region was accompanied by collision-related uplifting and simultaneous large-scale relief erosion, which resulted in the exposure of Late Miocene–Early Pleistocene minor granitoid intrusions (Chernyshev et al., 2006; Lebedev et al., 2009, etc.). Up to a few km-thick sections of these, frequently polyphase bodies are available for study in the gorges of large rivers taking their origin on the northern slope of the Main Caucasus Range. Such exposures are very rarely observed in modern volcanically active regions. For this reason, the young intrusions of the Greater Caucasus represent unique geological objects for petrological and isotope studies. The young age of the granitoids and, correspondingly, small absolute errors (usually tens to a few hundreds of thousand years) of obtained datings make it possible to determine such important characteristics of intrusive magmatism as the emplacement duration of granitoid massifs of different size, polyphase or monophase injection of magma, cooling rates of whole plutonic bodies and their individual blocks, and scales of a contact thermal effect on the isotope systems of different mineral phases of host rocks.

† Deceased.

The young intrusive bodies (so-called "neointrusions", Belyankin, 1924) of the Greater Caucasus occur in four spatially separated areals. The first areal spans the Caucasian Mineral Waters region with the Late Miocene mildly-alkaline granitoid magmatism (around 8 Ma, Pohl et al., 1883; Lebedev et al., 2006a). This pulse of the Late Cenozoic endogenous activity is the earliest among young magmatic manifestation of the Greater Caucasus. The second areal is located in the southern part of the Elbrus neovolcanic area confined to the Peredovoy Range zone and includes granite massifs (Eldzhurtu and others) with an age from 2.8 to 1.8 Ma (Hess et al., 1993; Gazis et al., 1995; Chernyshev et al., 2011).

The third, largest areal of the young intrusive magmatism is restricted to the Main Caucasus fault zone (upthrow fault) in the axial part of the Greater Caucasus. Its western part is traced from the Kvemo Svaneti–Zemo Racha (Georgia) and comprises several small Pliocene intrusive and subvolcanic bodies (Tsurungal, Karobi, and others) united by some authors in the Tsana Complex (for instance, Dokuchaev et al., 2013). Further eastward, the considered magmatic areal as a narrow band extends along the Bokovoy Ridge through North Ossetia and includes the Late Pliocene (around 2 Ma-old) Bartuidon, Songutidon, and Tepli granodiorite massifs (Tepli Complex) (Borsuk, 1979). The Dzhimara polyphase granodiorite-quartz diorite massif is exposed near Kazbek Volcano. This massif was formed in four magmatic pulses in the Pliocene (3.5–2.0 Ma) (Lebedev et al., 2009). The Kalkva hypabyssal dacitic massif dated at Early Pleistocene (ca. 1.4 Ma, Lebedev et al., 2016) is constrained to the junction zone of the Bokovoy and Main Caucasus ranges, near the Arkhoti pass in Khevsureti. It should be noted that numerous necks and hypabyssal dikes of intermediate-moderately acid rocks are distributed over the western and central parts of the described zone. It was shown (Lebedev et al., 2016) that some of these, mainly dacite and hyalodacite bodies (mountainous part of North Ossetia and Racha) were emplaced simultaneously with the Kalkva Massif. However, some of the above mentioned neointrusions may have earlier, Pliocene age.

The fourth areal of young intrusive magmatism is situated on the southern slope of the Greater Caucasus in the Kvemo Racha, near the foothills of Lelaashkha Mount (Central Georgian neovolcanic area). This area contains the series of the Late Miocene dacite dikes with an age of 7–6.5 Ma (Lebedev et al., 2013), which were emplaced simultaneously with manifestation of basic volcanism located slightly southerly in the same part of Georgia (Lebedev et al., 2006b). No dacitic bodies of similar age have yet been found in this part of the Greater Caucasus.

Geology and geochronology of young intrusions in different parts of the Greater Caucasus have been studied to different extent. Detailed structural description using surface and core samples with distinguishing intrusive phases, a great body of petrological-geochemical data, and thermochronological modeling are available for the best studied Eldzhurtu Massif in the vicinity of Tyrnyauz (Borsuk, 1979; Hess et al., 1993; Sobolev and Kononov, 1993; etc.). Only few geochemical data (Bogina, 1994) and K-Ar ages (Borsuk, 1979) were reported for the granitoid bodies of the Tepli Complex in North Ossetia. The exception is the Dzhimara Massif, whose evolution and genesis of parental magmas were deciphered by (Lebedev et al., 2009). New geochemical and geochronological data were recently obtained on the Kalkva dacite massif (Lebedev et al., 2016). At the same time, the neointrusions of the Tsana Complex, in particular, their age and petrogenesis, remain poorly studied, in spite of their inferred genetic link with previously exploited Mo and As deposits. It should be noted, first geological and petrographic data on the rocks of the complex have been published by Soviet geologists as early as mid-20th century (Ershov and Kopeliovich, 1937; Ershov, 1938; 1940; Kiknadze, 1967; Kharashvili, 1940), but modern high-precision techniques practically have not yet been applied to these objects.

The origin of the young granitoid massifs of the Greater Caucasus remains hotly debatable. Different petrogenetic models have been proposed to explain the evolution of acid intrusive magmatism in this region. In particular, Koronovskii and Demina (2007) consider the Pliocene neointrusions as purely crustal rocks derived by anatectic crustal melting in the collisional zone during large-scale regional compression coupled with heating of continental lithosphere. Borsuk (1979) and Pohl et al. (1993) ascribed the mildly-alkaline granites of the Caucasian Mineral Waters to A-type granites of mixed mantle–crustal origin. In contrast, Dubinina et al. (2010) believe that these massifs were derived from crustal felsic melts that assimilated carbonate material under subsurface conditions. Mixed mantle–crustal origin of granodiorites of the Tepli Complex proposed by (Bogina, 1994) was later confirmed by our studies (Lebedev et al., 2009). It was generally accepted in our recent works dedicated to the young magmatism of the Greater Caucasus (Chernyshev et al., 2006; Lebedev et al., 2009; 2014, etc.) that most of the Neogene–Quaternary igneous rocks of the region are hybrid in origin and their parental magmas were derived by (1) mixing of deep mantle melts with partial melts of crustal protolith, or (2) assimilation of crustal material by primary mafic magmas. The relative proportions of crustal and mantle components in the genesis of definite intrusive bodies or volcanic edifices widely vary in the different parts of the Greater Caucasus. It was also shown that the contribution of different sources in the petrogenesis of definite object (volcano/massif) could significantly change during period of its evolution (Lebedev et al., 2009; 2010).

In this paper, we discuss new isotope-geochronological data on the rocks of the Tsana Complex located in the central part of the Greater Caucasus at the adjacent territories of Georgia and Russia (North Ossetia). Obtained results allowed us to determine for the first time the affiliation of some young magmatic rocks to the Tsana Complex, to make conclusions about age and duration of the emplacement of plutonic and subvolcanic massifs, as well as the origin of the parental magmas of the granitods.

GEOLOGICAL POSITION OF THE INTRUSIVE BODIES OF THE TSANA COMPLEX

Small intrusive and subvolcanic bodies of the granitoids of the Tsana Complex are localized in the axial part of the Greater Caucasus, mainly in Georgia (Kvemo Svaneti and Zemo Racha) (Fig. 1). The massifs and associated numerous dikes are confined to the Main Caucasus fault zone, cutting across Paleozoic granite-metamorphic complexes of the Skythian plate to the north and Jurassic sedimentary sequences of the subduction-accretionary complex of the Southern slope of the Greater Caucasus to the south.

Recently, it is recognized two compact clusters with Pliocene neointrusions of the Tsana Complex, Tsurungal and Karobi, which are spaced at a distance of ~30 km in a sublatitudinal direction (Fig. 1). The Tsurungal group of intrusions is situated in the high-mountain part of the Kvemo Svaneti in the head waters of the right tributaries of the Tskhenistsqali–Koruldashi, Usakhelo, Chorokhi and Toteldash rivers (Fig. 2) on the southern slope of the Main Caucasus Range (Tsurungal Mount area). Plutonic bodies occur as small massifs of different composition and morphology and dikes cutting across Liassic shales and rarely Late Jurassic–Early Cretaceous carbonate sequence. Shales in the contact aureoles of the intrusions from few tens to 600–700 m were hornfelsed and overprinted by arsenopyrite mineralization (Tsana deposit). The largest massifs of the group are Tsurungal, Chorokhi, and Toteldash (Fig. 2). The Tsurungal Massif, up to 2.5 km^2 in area, was recovered south of Tsurungal Mount in the Zeskho River basin, between its right tributaries Koruldashi and Usakhelo (Karetta ridge), in the very inaccessible area at an altitude of 2800–3500 m. Morphologically, the Tsurungal Massif represents stock extended from SW to NW, with contacts steeply dipping at 50°–80° (Kiknadze, 1967). It is made up mainly of medium-grained biotite granite porphyry and less common porphyritic granite, while its marginal parts consist of granodiorite porphyry, monzogranite, quartz diorite, and diorite porphyry. No sharp contacts were found between different rock varieties; the granite porphyry and porphyritic granite are linked by transitional varieties. The massif is associated with numerous dikes (up to 15 m thick) of different composition, which strike sublatitudinally (280°–300°) and frequently sublongitudinally (60°–70° or 340°–350°) (Fig. 2). The dike bodies framing the Main Caucasus fault are characterized by larger thickness and more mafic composition (microdiorite, quartz diorite porphyry, diorite porphyry, and granodiorite porphyry). According to Kiknadze (1967), they were emplaced slightly earlier than the main granite porphyry stock: the apophyses of the latter frequently cut across the diorite dikes, displacing them. In turn, the Tsurungal Massif is cut by small submeridionally oriented dikes of leucocratic granite and granite porphyry usually within 2–3 m thick, and by aplite and pegmatite veins.

The Chorokhi Massif is situated in the heads of the eponymous river, where it intrudes the Liassic shales. It represents a small stock 150 × 300 m in exposed size with steeply (70°–80°) dipping contacts (Fig. 2). The massif is made up of two-mica granite, which pass into granodiorite porphyry and monzogranite in the endocontact zones. The transitions between the rocks are gradual, without intrusive relations. The Toteldash granite porphyry stock is exposed in the upper reaches of the eponymous river, on its left bank, and has even lesser size (50 × 60 m) (Fig. 2). It cuts across a sublatitudinal granodiorite porphyry dike up to 10–15 m thick, with magmatic breccia in the contact zone.

Three intrusive phases were distinguished by Kiknadze (1967) from study of geological relationships between different intrusive bodies of the Tsurungal Group. The first phase includes small massifs and sublatitidunal diorite–granodiorite dikes up to 6–7 km long. The second phase is represented by granite porphyry stocks, and the third phase, by the most silicic small leucogranite dikes and aplite veins. The author noted that the young magmatism of the region also shows basic to acid evolution, with small gaps between intrusive phases, as follows from relations of different magmatic bodies with the same tectonic structures.

The emplacement of the neointrusions of the Tsurungal group is likely associated with the formation of base metal and Sb-arsenopyrite mineralization. The economic reserves of the ores are known at the Tsana deposit and at some small objects around it. The Tsana deposit mined in mid-20th century is described in detail in (Ershov and Kopeliovich, 1937; Ershov, 1938, 1940). It is presently considered as promising object for gold extraction from arsenopyrite ores and now is being prepared for repeated exploration.

The Karobi group of intrusions is localized in the Zemo Racha, in the head waters of the Chashuri River (Rioni River basin) near the Kirtisho glacier (Figs. 1, 3, 4). According to (Kharashvili, 1940), the Karobi ridge comprises two subvolcanic bodies and a thick rhyodacite dike, as well as numerous NS-trending dike bodies of plagiophyric trachyandesite ("albitophyre", according to the cited author). The largest rhyodacite massif around 0.2 km^2 in area is situated on the left bank of the Chashuri River, 1 km downstream

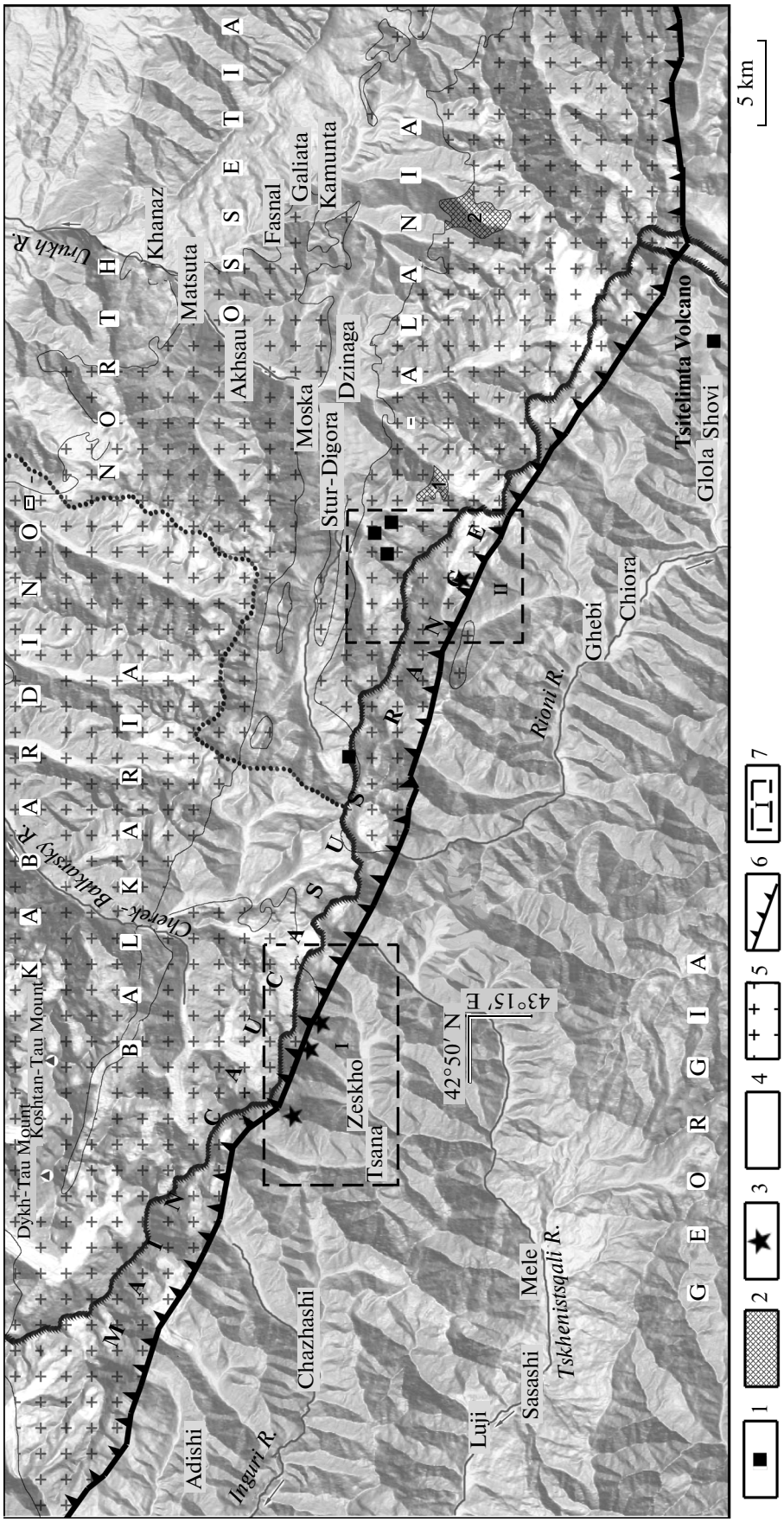

Fig. 1. Orographic map of the central part of the Greater Caucasus with indication of areas of Pliocene intrusive magmatism. (1) Pleistocene volcanic vents, (2) Late Pliocene granitoid massifs ((1) Bartuidon, (2) Songutidon), (3) Early Pliocene intrusive massifs, (4) Mesocenozoic volcano-sedimentary cover, (5) exposed Paleozoic crystalline basement, (6) Main Caucasus Fault (upthrow fault), (7) studied areas ((I) Tsurungal Group, (II) Karobi Group).

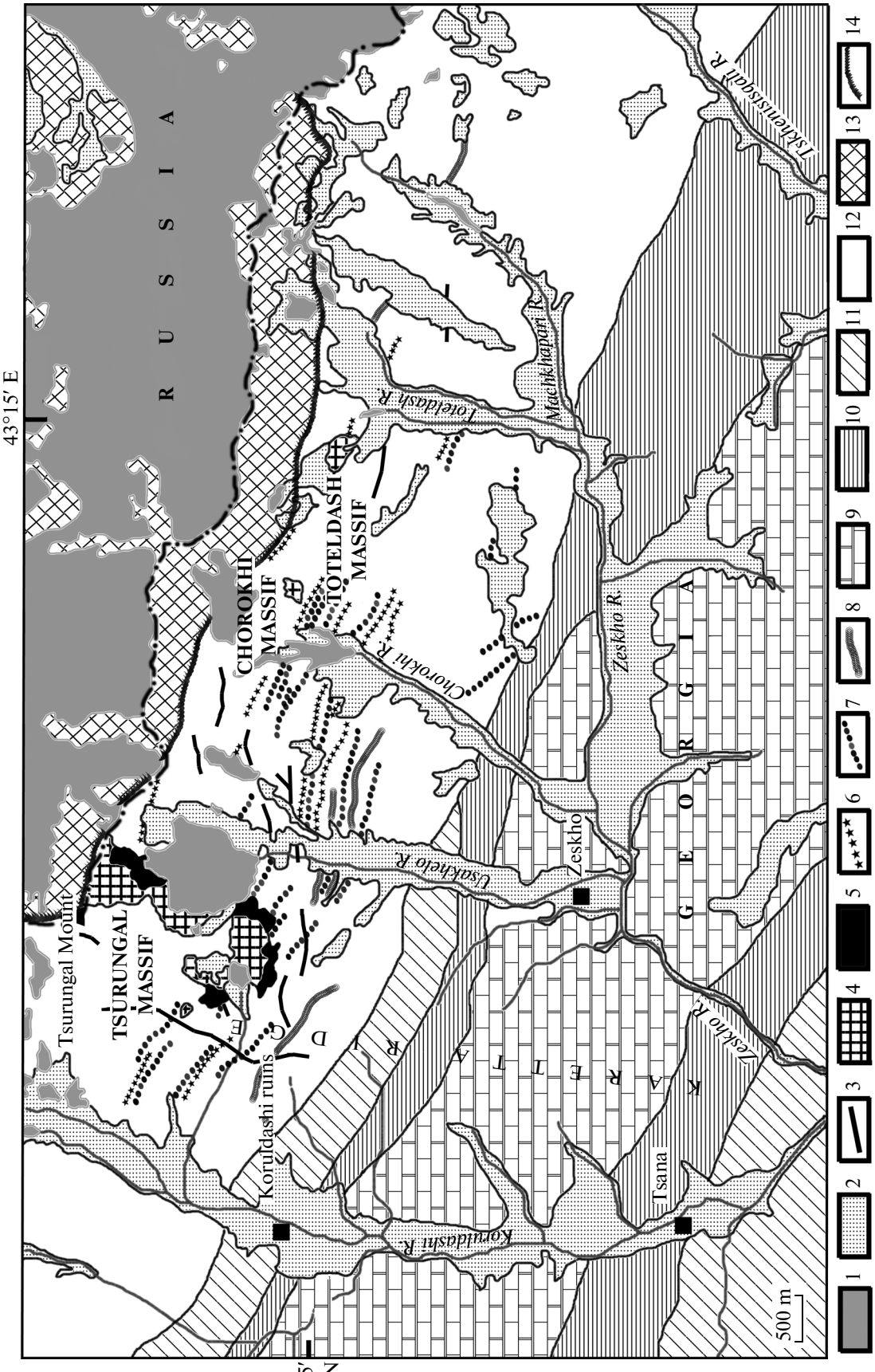

Fig. 2. Geological map showing the distribution of the Early Pliocene granitoid intrusions of the Tsurungal group. Compiled using materials by Kiknadze (1967) and deciphering detailed satellite images. (1) Glaciers and firn fields in 2010, (2) Quaternary sedimentary rocks, (3–8) Early Pliocene magmatic rocks of the Tsana intrusive complex: (3) leucocratic granite, quartz porphyry, and aplite dikes of phase III, (4) granite porphyry, porphyritic granite, and two-mica granites of phase II, (5) granodiorite porphyry, monzogranite, quartz diorite porphyry, and diorite porphyry of phase I, (6) granodiorite dikes of phase I, (7) diorite porphyry and quartz diorite porphyry dikes of phase I, (8) microdiorite and quartz microdiorite dikes of phase I; (9) Early Cretaceous limestone, marl, and shale (Chiora and Porkhishuli formations), (10) Late Jurassic limestone, marl, sandstone, and conglomerate (Notsarula and Chvesshura formations), (11) Middle Jurassic clayey—sandy shale and sand (Talakhiani Formation), (12) Early Cretaceous slate and shale, sandstone, and sheeted diabase veins (Muashi and Morgouli formations), (13) Paleozoic granite-metamorphic basement complexes of the Greater Caucasus, (14) Main Caucasus fault (upthrow fault).

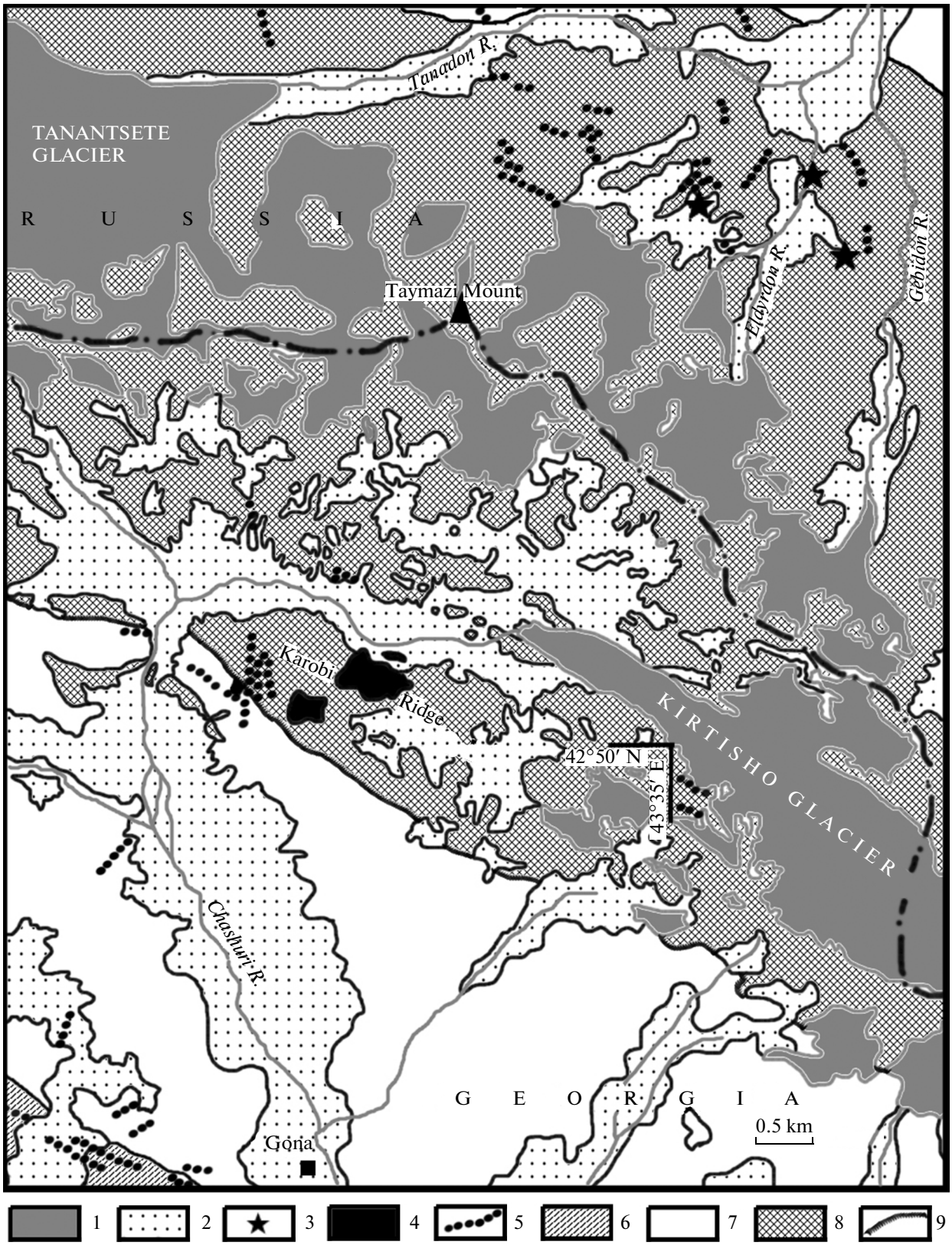

Fig. 3. Geological map showing the distribution of the Early Pliocene intrusions of the Karobi Group. Compiled using data from (Kharashvili, 1940; Konstantinov et al., 2005). (1) Glaciers and firn fields in 2010, (2) Quaternary sedimentary rocks, (3) Early Pleistocene volcanic vents, (4–5) magmatic rocks of the Early Pliocene Tsana intrusive complex: (4) intrusive rhyodacite massifs, (5) trachyandesite dikes, (6) Middle Jurassic sandstone and shale (Sori Formation); (7) Early Jurassic slate and shale, sandstone, sheeted diabase veins (Muashi and Morgouli formations), (8) Paleozoic granite-metamorphic basement complexes, (9) Main Caucasus Fault (upthrow fault).

Fig. 4. Upper reaches of the Chashuri River, near the Kirtisho glacier. Exposures of the Karobi rhyodacite neointrusion are seen on the right side of the photo.

of the Kirtisho glacier edge (Fig. 4). This neointrusion has cross-cutting relations with host Paleozoic mylonitized granite gneisses and thin (6–7 m) outer contact aureole. The second smaller rhyodacite body is situated 600–700 m south of the crest part of the Karobi ridge and consists of the rocks of similar composition and petrographic appearance. The rhyodacite dike of small extension cutting across early plagiophyric trachyandesite neointrusions is known on the southern slope of this ridge. In terms of the petrographic appearance, the holocrystalline rocks of this dike are close to granite porphyry. Its outer contact bears molybdenite mineralization (Karobi deposit), which was intensely exploited during the World War II. The magmatic bodies of the Karobi group are also associated with arsenopyrite and sulfide-base metal mineralization (Kharashvili, 1940).

Data by Kharashvili (1940) indicate that the neointrusons of the Karobi group were formed in two magmatic phases: (1) emplacement of "albitophyre" dikes and (2) formation of the later rhyodacite bodies, cutting the dikes. In author's opinion, these pulses of endogenic activity were separated by a small age interval, and igneous rocks of both phases presumably were "derivatives of the same magmatic chamber".

It is pertinent to mention that the NS-trending plagiophyric trachyandesite dikes similar to those described in the upper reaches of the Chashuri River are also exposed on the northern slope of the Main Caucasus Range on the territory of North Ossetia (head waters of the Tanadon River, the left tributary of the Urukh River), only few kilometers north of the Karobi ridge (Fig. 3). These intrusive bodies cutting across Paleozoic granitoids of the Skythian plate were mentioned by Konstantinov et al. (2005) while describing the Tanadon Au-arsenopyrite deposit. It is noteworthy that later volcanic activity in this area also occurred (end of the Pliocene–early Pleistocene) in two pulses: around 2.5–2.0 and 1.4 Ma (Lebedev et al., 2016). The first pulse was responsible for the formation of a granodiorite massif near the Bartui glacier (Tepli Complex), while the second pulse produced several necks in the upper reaches of the Tanadon River and near the Zopkhito glacier, as well as numerous sublatitudinal thin dacite-hyalodacite dikes at the mountainous part of North Ossetia and Zemo Racha (Figs. 1, 3). Thus, the distribution areal of the Pliocene magmatism of the Tsana Complex in its eastern part is overlapped with the areal of later (Pliocene–Early Quaternary) Tepli Complex.

The close geographic position of the plagiophyric trachyandesite dikes in the upper reaches of the Tanadon River with compositionally and petrographically similar dikes of the Zemo Racha, and, as will be shown below, with simultaneous young subvolcanic rhyodacite massifs in this region allow us to unite all above mentioned subvolcanic bodies in a single Karobi neointrusion group.

The Pliocene age of the intrusive bodies of the Tsana Complex was established in the mid-20th cen-

Table 1. Results of K-Ar dating of the Pliocene magmatic rocks of the Greater Caucasus

Sample	Mineral	Potassium, % ±σ	$^{40}Ar_{rad}$, ng/g ±σ	$^{40}Ar_{air}$, % in sample	Age, Ma ±2σ
Tsurungal group					
M-223, granite porphyry	Biotite	7.50 ± 0.08	2.124 ± 0.015	68.1	4.08 ± 0.10
	Groundmass	5.15 ± 0.06	1.331 ± 0.013	56.5	3.72 ± 0.11
LSh-1, porphyritic granite	Biotite	7.61 ± 0.08	2.230 ± 0.012	63.4	4.22 ± 0.10
	K-Fsp	9.85 ± 0.10	2.660 ± 0.011	30.6	3.89 ± 0.09
M-174, quartz diorite porphyry	Rock	1.45 ± 0.02	0.52 ± 0.03	55.7	5.2 ± 0.4
Karobi Massif					
R-196, rhyodacite	Groundmass	2.63 ± 0.03	0.863 ± 0.011	55.2	4.72 ± 0.16
	Biotite	4.92 ± 0.05	1.57 ± 0.04	46.6	4.60 ± 0.25
R-200, rhyodacite	Biotite	6.69 ± 0.07	2.284 ± 0.016	30.2	4.91 ± 0.12
R-358, rhyodacite	Groundmass	2.57 ± 0.03	0.922 ± 0.013	57.3	5.15 ± 0.20
	Biotite	7.14 ± 0.08	2.37 ± 0.02	45.9	4.78 ± 0.14
Dikes in the upper reaches of the Tanadon River					
Ur-21, trachyandesite	Groundmass	2.02 ± 0.03	0.674 ± 0.006	54.7	4.80 ± 0.17
Ur-24, trachyandesite	Groundmass	1.96 ± 0.02	0.630 ± 0.004	63.6	4.63 ± 0.11

Table 2. Results of Rb-Sr dating of the Pliocene magmatic rocks of the Greater Caucasus

Sample	Mineral	Rb, ppm	Sr, ppm	$^{87}Rb/^{86}Sr$ ±2σ	$^{87}Sr/^{86}Sr$ ±2σ
Tsurungal Massif					
M-223	Biotite	566	5.5	299.2 ± 8	0.725103 ± 16
	Groundmass	178	247	2.087 ± 6	0.707259 ± 9
	Plagioclase	21	480	0.1279 ± 5	0.706053 ± 10
Karobi Massif					
R-358	Biotite	147	4.5	92.3 ± 4	0.711451 ± 25
	Groundmass	80	186	1.270 ± 4	0.705329 ± 10
	Plagioclase	4.0	1080	0.0108 ± 3	0.705025 ± 10

tury by K–Ar dating of two biotite fractions from the Tsurungal and Karobi granitoid massifs performed at the Institute of Geology of Ore Deposits, Petrography, Mineralogy, and Geochemistry, Russian Academy of Sciences (Borsuk, 1979). These, first obtained isotopic-geochronological data confirmed the Neogene age previously suggested for the Complex from geological observations (Kharashvili, 1940; Kiknadze, 1967; etc.). However, the measurement accuracy at that time was insufficient to determine reliably the total duration of this magmatic pulse, differences in the age of the individual phases, and synchronous/asynchronous formation of the Tsurungal and Karobi groups. The solution of this problem became the main aim of this study.

ANALYTICAL METHODS

Isotope dating of the Pliocene magmatic rocks of the Greater Caucasus was carried out by K-Ar and Rb-Sr methods. Monomineral fractions (biotite, *Kfs*) and groundmass extracted from the studied granitoids and subvolcanic rocks were used as analyzed material. Results are presented in Tables 1 and 2.

The concentration of radiogenic Ar in each sample was analyzed on a MI-1201 IG (SELMI) mass spectrometer by isotope dilution using ^{38}Ar monoisotope as spike, while the concentration of potassium content was measured by flame spectrophotometry on an FPA-01 photometer (Elam Center). The measurement accuracy was controlled by systematic analyses

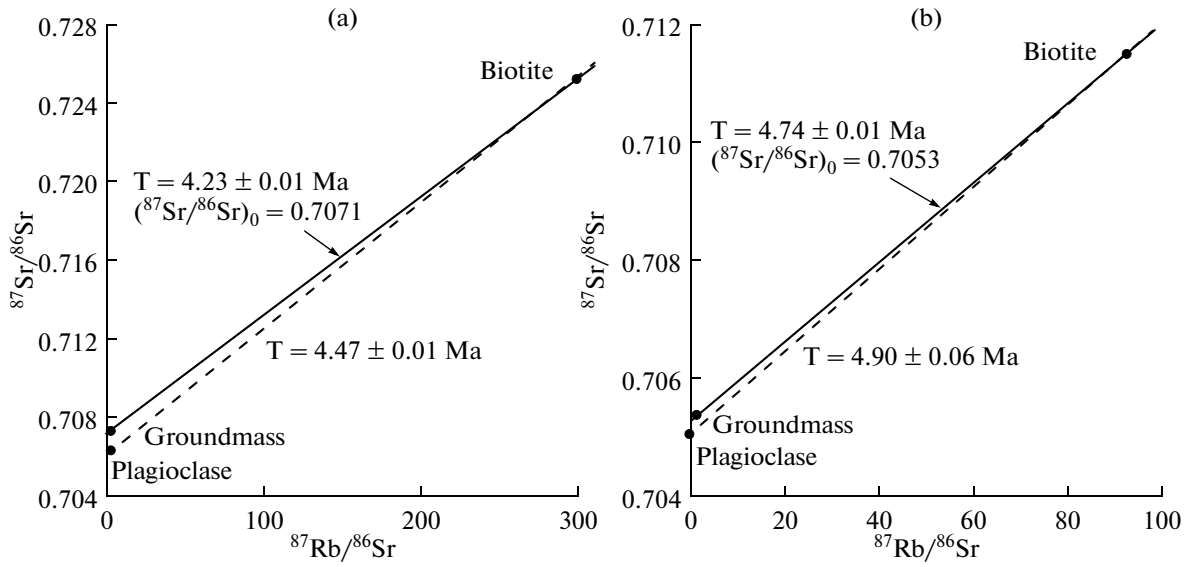

Fig. 5. Rb-Sr isotope diagrams for samples M-223 (granite porphyry from the Tsurungal Massif) (a) and R-358 (rhyodacite from the Karobi Massif) (b).

of muscovite "Bern-4" and rhyolite "Asia" standards and atmospheric argon. The characteristics of the applied technique and principles of calculation of final age uncertainties are given in (Chernyshev et al., 2006).

The Rb and Sr concentrations in different components of the studied rocks for Rb-Sr dating were determined using an isotope dilution technique. Isotope ratios were measured on a Micromass Sector 54 multicollector TIMS (Thermo Scientific). The measurements were controlled by the systematic analysis of SRM-987 International standard. The $^{87}Sr/^{86}Sr$ and $^{87}Rb/^{86}Sr$ isotope ratios in the studied samples were measured with accuracy of 0.003 and 0.3–2.7%, correspondingly.

Isotope ages were calculated using the International decay constants for potassium and rubidium (Steiger and Jager, 1977).

The chemical composition (rock-forming oxides) of the Pliocene magmatic rocks of the Greater Caucasus was analyzed by XRF method at the Institute of Geology of Ore Deposits, Petrography, Mineralogy, and Geochemistry, Russian Academy of Sciences (analyst A.I. Yakushev) using an Axios mAX (PANalytical, the Netherlands) wavelength dispersive vacuum sequential spectrometer.

RESULTS AND DISCUSSION

Results of Isotope-Geochronological Studies

The K-Ar and Rb-Sr dating was performed for different components of the granitoids of intrusive and subvolcanic bodies of the Tsurungal and Karobi groups (Tables 1 and 2).

For the Tsurungal group, the K–Ar ages were obtained for quartz diorite porphyry dike [sample M-174, phase I according to (Kiknadze, 1967)] in the upper reaches of the Zeskho River, as well as for granite porphyry (sample M-223) and porphyritic granites (sample LSh-1) from the Tsurungal Massif [phase II according to (Kiknadze, 1967)]. Sample M-223 was dated by Rb-Sr method on biotite–groundmass–plagioclase triad (Table 2, Fig. 5).

Obtained results, at first, confirm the Early Pliocene age (5–4 Ma) of the plutonic bodies of the Tsurungal group, and, second, indicate that the intrusive phases I and II were separated by a significant time gap. The K-Ar age of the earlier quartz diorite porphyry dike corresponds to 5.2 ± 0.4 Ma. Two monomineral biotite separates (purity >99%) from later granites yield similar (within analytical error) dates averaging 4.15 ± 0.10 Ma. Mainly feldspar groundmass from sample M-223 and *Kfs* from sample LSh-1 define slightly younger K-Ar ages from 3.9 to 3.7 Ma. This fact may be explained by either (1) the later closure of the K-Ar isotope system in K-feldspar as compared to biotite at sufficiently slow cooling of granitic bodies (as known, the biotite K-Ar closure temperature is much higher than that of the low-temperature *Kfs* varieties), or (2) partial loss of radiogenic ^{40}Ar by feldspar during its postmagmatic structural rearrangement. The inferred rapid cooling of the massifs owing to their small sizes gives grounds to consider the second variant as more plausible. This is also confirmed by decomposition and pelitization of feldspars observed during petrographic study of the rocks. In any case, K–Ar biotite datings are more preferable as more reliable estimates of the formation age of the granitoids.

The Rb-Sr plagioclase-biotite-groundmass dating of granite porphyry of the Tsurungal Massif (sample M-223) (Table 2) revealed that the rock components with low Rb/Sr ratio are characterized by different initial Sr isotope composition, which makes it impossible to plot the three-point isochrone (Fig. 5). The Rb-Sr biotite-plagioclase age is 4.47 ± 0.01 Ma, while the Rb-Sr biotite-groundmass age is 4.23 ± 0.01 Ma. It is obvious, the last value within calculated uncertainties coincides with the K-Ar biotite age of the granites of the Tsurungal Massif, which suggests that the Rb-Sr biotite–groundmass system reached equilibrium and defines the age of real geological event. At the same time, Rb-Sr biotite–plagioclase dating is much older, while the initial Sr isotope composition of feldspar is less radiogenic as compared to that of the groundmass: $(^{87}Sr/^{86}Sr)_0$ are 0.7061 and 0.7071, respectively. We suggest that the Rb-Sr system of this mineral pair did not reach equilibrium, which is primarily related to the isotopic heterogeneity of zoned plagioclase phenocrysts. The petrographic study of the Tsurungal granitoid massif (Table 3) indicates that plagioclase in these rocks forms two or three generations, which demonstrate different types of zoning and were presumably formed at different stages of the evolution of magmatic melt during significant change of its geochemical, including isotope characteristics. For instance, the cores of the early plagioclase phenocrysts (with normal zoning) correspond to labradorite (An 55-60), whereas their inner rims are oligoclase (An 18-20). The central parts of such phenocrysts may "conserve" plagioclase that initially crystallized from equilibrium basic or intermediate melt in the deep-seated magma chamber. Later changing of petrological-geochemical characteristics of magma in the shallow chamber, the possible mechanisms and reasons of which will be considered below, led to the formation of more sodic rim with different Sr isotopic composition around the calcic core. Thus, considered feldspar phenocrysts from the granitoids of the Tsurungal Massif may represent a complex heterogeneous mineral system with isotopically and chemically zoned structure. As a result, only later plagioclase from rims may be in isotope equilibrium with groundmass (melt) and biotite that crystallized at the final stages of magmatic evolution, while plagioclase from the inner zones has distinct lower Sr ratio. In this connection, Rb-Sr age determination (4.47 ± 0.01 Ma) on biotite and mixture of plagioclases of different generations, when feldspar demonstrates clearly expressed Sr isotopic heterogeneity, is geologically meaningless and does not correspond to any geological event. In contrast, the Rb-Sr biotite–groundmass age (4.23 ± 0.01 Ma), coinciding with the K-Ar biotite age on the Tsurungal granite porphyry massif, may be considered as the independent confirmation of the reliability of the latter. It should be noted that the similar evidences for isotope heterogeneity in the young Caucasian granitoids were obtained during Rb-Sr biotite–groundmass–plagioclase dating of rhyodacite from the Karobi Massif (Fig. 5) and, earlier, for subvolcanic dacites from a Quaternary Kalkva massif in Khevsureti (Lebedev et al., 2016). Thus the age of phase II granitoids of the Tsurungal intrusions is taken to be 4.15 ± 0.10 Ma. This value coincides, within error, with estimating dating of 4.0 ± 0.2 Ma obtained for granite porphyry of the Tsurungal Massif in the mid-20th century at the Institute of Geology of Ore Deposits, Petrography, Mineralogy, and Geochemistry, Russian Academy of Sciences (Borsuk, 1979), and allows us to refine the age of this plutonic body.

The analysis of obtained isotope–geochronological data allowed us to establish that the rocks of the Tsurungal group were formed during two different pulses of magmatic activity: around 5 and 4 Ma. The first stage produced dikes and small stocks of diorite porphyry and granodiorite [magmatic phase I according to Kiknadze (1967)], while phase II was responsible for the formation of small granitic stocks, as well as cross-cutting dike leucogranite bodies and aplite veins (phases II and III according (Kiknadze, 1967)). The time gap between two mentioned pulses of intrusive magmatism may account for over 500 ka.

Five K-Ar dates were obtained with biotite–groundmass pair (Table 1, samples R-196, R-200, R-358) from rhyodacite dike on the southern slope of the Karobi Ridge. The altered biotite (opacitization and hydration) from sample R-196 with low K content in mica (<5 wt %) defines the minimum age, which differs from other isotope datings and may be excluded from consideration. Other four K-Ar ages fall in a narrow range from 4.72 to 5.15 Ma, coincide within measurement error, and yield a weighted average value of 4.80 ± 0.15 Ma. The biotite-groundmass pair from sample R-358 yields practically the same Rb-Sr age of 4.74 ± 0.01 Ma (Table 2, Fig. 5). At the same time, the biotite-plagioclase pair defines somewhat older Rb-Sr age of 4.90 ± 0.06 Ma, which, however, also coincides within error with the K-Ar age. The overestimated Rb-Sr age of this pair is possibly explained by the same reasons as discussed above for isotope dating on the granite porphyry of the Tsurungal Massif.

The coincidence of the K-Ar and Rb-Sr dates on the rhyodacite from the Karobi Massif allowed us to accept the value of 4.80 ± 0.15 Ma as the reliable geological age of this subvolcanic body. It should be noted that this age is somewhat older than the estimating K-Ar dating of 4.3 ± 0.2 Ma published in (Borsuk, 1979).

K-Ar dating on groundmass from two trachyandesite dikes (samples Ur-21 and Ur-24, Table 1) samples in the upper reaches of the Tanadon River, North Ossetia, made it possible to determine the narrow range of their formation within 4.8–4.6 Ma. This time interval completely coincides with our dates on the rhyodacite bodies from the Karobi ridge. Based on this fact in combination with close geographical position of the considered objects within the Greater Caucasus

Table 3. Main petrographic characteristics of the magmatic rocks of the Tsana Complex

Rock	Structural-tectonic features	Proportions of phenocrysts and groundmass, vol %	Mineral composition	Subordinate and accessory minerals
Tsurungal group Phase I *Dike and Vein rocks*				
Microdiorite	I, 1, A	–	*Pl* (no. 50-23)—63–65%, *Bt*—34%	*Qz* <1%. *Ap*, *Spn*, *Mag*, *Zrn*
Quartz microdiorite	I, 1, A	–	*Pl* (no. 50-23)—60–63%, *Bt*—24–25%, *Qz*—9–11%	*Ap, Spn, Mag, Zrn*
Diorite porphyry	II, groundmass—1-2, A, D (sometimes)	20-25/72-76	Phenocrysts: *Pl* (no. 60-20, averaging no. 38-30, zon)—15–20%, *Bt*—5–7%. Groundmass: *Pl* (*An* 28-20), *Bt*, *Qz*.	Phenocrysts: *Qz* < 0.5%, *Kfs* <0.5%. *Ap*, *Spn*, *Mag*, *Zrn*, *Tur*
Quartz-bearing diorite porphyry	II, groundmass—1-2, A	22-25/65-76	Phenocrysts: *Pl* (no. 60-20, on average—*An* 38-28, zon)—6–17%, *Bt*—4–12%. Groundmass: *Pl* (no. 28-10), *Bt*, *Qz*, *Kfs*	Phenocrysts: *Qz*—1–4%, *Kfs*—0–10%. *Ap, Spn, Zrn, Tur*
Granodiorite porphyry	II (rarely I or III), groundmass—1-2, A, B (sometimes)	35-40/51-62	Phenocrysts: *Pl* (no. 50-15, on average *An* 30-18, zon, gl)—11–17%, *Kfs* (*Ano*)—5–18%, *Qz*—2–11%, *Bt*—2–9%. Groundmass: *Qz, Pl* (no. 23-10), *Bt, Kfs*	*Ap*—1–3%, *Spn, Zrn, Tur*
Massif rocks				
Granodiorite porphyry	II (sometimes I, rarely III), groundmass—2, A	40/60	Phenocrysts: *Pl* (no. 60-21, on average—no. 42-19, zon, gl), *Qz*, *Bt*. Groundmass: *Pl* (no. 23-18), *Kfs* (*Ano*)—17–19%, *Qz*, *Bt*. In total: *Pl*—37–50%, *Qz*—20–31%, *Kfs*—17–19%, *Bt*—8–10%	*Ap*—2–3%, *Zrn*—0.5–1%, *Spn, Tur, Mag, Cst*
Monzogranite	I (rarely II), 2, A	–	*Pl* (no. 40-10)—33%, *Kfs* (*Ano*)—30, *Qz*—25%, *Bt*—10%	*Ap*—1%, *Zrn, Spn, Tur, Mag*
Quartz diorite porphyry	II, groundmass—1-2	20-25/70-75	In total: *Pl* (no. 60-20)—64%, *Bt*—19%, *Qz*—11–12%	*Kfs* <5%. *Ap*—1.5%, *Zrn, Spn, Mag*
Diorite porphyry	II, groundmass—1-2	20-25/70-75	In total: *Pl* (no. 60-20)—64%, *Bt*—31%	*Qz*—< 0.5%, *Kfs* <1.5%. *Ap*—3%, *Zrn, Spn, Mag*

Table 3. (Contd.)

Rock	Structural-tectonic features	Proportions of phenocrysts and groundmass, vol %	Mineral composition	Subordinate and accessory minerals
		phase II *Massif rocks*		
Granite porphyry	II, groundmass—1, A, E	40/60	In total: *Kfs* (*Ano-Mc*)—36%, *Qz*—33%, *Pl* (phenocrysts—An 55-15, on average *An* 25-20, zon; groundmass An 21-19)—22%, *Bt* (phenocrysts—6–12%, groundmass—1–2%)	Phenocrysts: *Amp* <1–2%. *Ap*—3.0–0.5%, *Zrn*—1.0–0.5%, *Mnz, Spn, Mag, And, Tur*
Porphyrytic granite	II (rarely I), groundmass—2, A	40/60	In total: *Kfs* (*Ano-Mc*)—36%, *Qz*—31%, *Pl* (no. 30-10, zon)—23%, *Bt*—8%	*Ap*—1%, *Zrn, Spn, Tur, Mag*
Two-mica granite	I (rarely, II), 2, A	–	*Kfs* (*Ano-Mc*)—37%, *Qz*—29%, *Pl* (no. 29-19, zon)—21%, *Ms*—6%, *Bt*—6%	*Zrn*—0.5%, *Ap*—0.5%, *Tur, Spn, Cst, Mag*
		Phase III *Dike and vein rocks*		
Granite porphyry	II, groundmass—1-2, A	40/60	In total: *Qz*—39%, *Kfs* (*Ano-Mc*)—31%, *Pl* (phenocrysts—no. 27-20, zon; groundmass—no. 21-10)—19%, *Bt*—8%	*Ap, Zrn, Tur, Spn, Rt, Mag*
Leucocratic granite	I, 1-2, A	–	*Kfs* (*Ano-Mc*)—38%, *Qz*—36%, *Pl* (no. 21-10, zon)—21%	*Bt* < 4%. *Ap, Zrn, Tur, Spn, Rt, Mag*
Quartz porphyry	II, groundmass—1, F (rarely G)	40/60	In total: *Qz*—40–36%, *Kfs* (*Ano*)—32–30%, *Pl* (no. 25-10, zon)—25–22%, *Bt*—7–5%	*Ms* <1%. *Zrn, Tur, Ap, Spn, Mag*
Aplite	V (rarely II)	–	*Kfs* (*Ano*)—40%, *Qz*—32%, *Pl* (An 18-10)—23–22%	*Bt* <2.5%, *Ms* <1%. *Zrn, Ap, Tur, Cst, And, Grt*
		Karobi group *Massif rocks*		
Rhyodacite	IV, groundmass—B	50/50	Phenocrysts: *Pl* (andesine, zon)— 40%, *Qz*—5%, *Bt*—5%. Groundmass: *Qz, Pl, Bt*	*Mag, Ap, Zrn*
		Dike rocks		
Trachyandesite	II (sometimes IV), groundmass—H	15-20/80-85	Phenocrysts: *Pl* (no. 35, zon)—8–10%, *Qz*—6–7%, *Amp*—4–6%. Groundmass: *Pl, Amp*	*Bt* <1%, *Cpx* <1%, *Ol* <1%. *Spn, Ap, Mag*

Author's data and data from monograph (Kiknadze, 1967).

Structural-textural features: (I) equigranular, (II) porphyrytic or porphyraceous, (III) taxitic, (IV) glomeroporphyric, (V) aplite-like or aplitic. (1) fine-grained, (2) medium-grained, (A) hypidiomorphic, (B) granophyric, (C) microallotriomorphic, (D) fluidal, (E) microgranitic, (F) micropegmatitic, (G) felsitic, (H) panidiomorphic. Minerals: (*Amp*) amphibole, (*And*) andalusite, (*Ano*) anorthoclase, (*Ap*) apatite, (*Bt*) biotite, (*Cpx*) clinopyroxene, (*Cst*) cassiterite, (*Grt*) garnet, (*Kfs*) potassium feldspar, (*Mc*) microcline, (*Mag*) magnetite, (*Ms*) muscovite, (*Mnz*) monzonite, (*Ol*) olivine, (*Pl*) plagioclase, (*Qz*) quartz, (*Rt*) rutile, (*Spn*) sphene, (*Tur*) tourmaline, (*Zrn*) zircon, (zon) zonal crystals, (gl) glomerophyric intergrowths.

mountain system, the NS-trending dikes of plagiophyric trachyandesite ("albitophyre") may be ascribed to the Tsana rather than to the Tepli intrusive complex, as earlier suggested by some researchers (Konstantinov et al., 2005), and may be included in the Karobi group of intrusions. Thus, our data confirm previous conclusion by Kharashvili (1940) that the young subvolcanic rhyodacite bodies of Zemo Racha were formed simultaneously with "albitophyre" dikes distributed in this area.

Analysis of obtained isotope-geochronological data allowed us to draw the main chronological regularities in the evolution of the intrusive magmatism of the Tsana Complex. The subvolcanic and hypabyssal bodies of the Tsurungal group were formed at the Zanclean stage presumably during two discrete pulses of endogenic activity (around 5 and 4.15 ± 0.10 Ma), while the Karobi neointrusions were formed during one pulse (4.80 ± 0.15 Ma). Within error, the age of the phase-I rocks of the Tsurungal group coincides with the age of the massifs and dikes of the Karobi group. In our opinion, they mark the same initial pulse of the Early Pliocene activity, which manifested simultaneously within both clusters of the Tsana granitoids. The greater amount and better accuracy of isotope dates obtained on the rocks of the Karobi group as compared to the single K-Ar estimate for early diorite porphyry of the Tsurungal group give grounds to take the age of 4.80 ± 0.15 Ma as the reliable age value for this pulse.

The second (later) magmatic pulse of the Early Pliocene Tsana complex (4.15 ± 0.10 Ma), determined by us for the Tsurungal group is related to the formation of small granitic bodies and veins. The bodies of this age were not found in the distribution area of the Karobi group. Thus, the earlier phase of the Early Pliocene magmatism of the Tsana Complex occurred simultaneously in different parts of its areal, while its final phase occurred only in the western part of this areal.

Isotope-geochronological data show that the young magmatism of the Tsana intrusive complex in the Early Pliocene lasted from 500 to 900 kyr within time interval from 4.80 ± 0.15 to 4.15 ± 0.10 Ma. This endogenic activity occurred as two clearly discrete pulses (phases) of magmatism separated by a time gap significantly exceeding the duration of these pulses.

Obtained results in combination with previously published isotope-geochronological data (Hess et al., 1993; Gazis et al., 1995; Lebedev et al., 2006b, 2009, 2010, 2013, 2016; Lebedev and Vashakidze, 2014; Chernyshev et al., 2006, 2011) provide insight into spatial migration of the magmatic activity at the Greater Caucasus from Late Miocene to the end of the Quaternary (Fig. 6). The first manifestations of the volcanic activity in the considered period occurred 7.2–6.0 Ma within the Central Georgian neovolcanic area on the southern slope of the Greater Caucasus and included both basic and intermediate–moderately-acid rocks (Lebedev et al., 2006b, 2013). Later, the endogenic activity migrated northward, in the zone of the Main Caucasus Range and was represented by the intermediate–felsic rocks of the Tsana neointrusions emplaced in the territory of modern Zemo Racha, Kvemo Svaneti, and mountainous part of North Ossetia (5–4 Ma). Further, magmatism migrated in two opposite directions: to the east and northwest. At the end of Pliocene-beginning of Pleistocene (from 3.5 to 1.4 Ma), the eastern areal represented a narrow band along the Main Caucasus and Bokovoy ranges, which extended from the Urukh River head in North Ossetia to the upper reaches of the Assa and Khevsuretis Aragvi rivers in the northeastern part of Georgia. At the end of the Pleistocene, the magmatic activity from the easternmost sector of this zone again migrated to the southern slope of the Greater Caucasus, where intermediate and moderately-acid volcanism formed the Kazbek and Keli neovolcanic centers in the upper reaches of the Terek, Aragvi, and Greater Liakhvi rivers during period from 400 ka to the Holocene (Lebedev and Vashakidze, 2014, etc.).

The second "vector" of lateral migration of the young activity at the end of the Neogene was directed from the manifestation area of the Tsana Complex to the northwest, in the upper reaches of the Chegem and Baksan rivers (Fig. 6). The Late Pliocene was marked by the formation of the large Chegem volcanic center (3.7–2.7 Ma, Gazis et al., 1995; Chernyshev et al., 2006) and to the west by younger (2.5–1.8 Ma) small granitic intrusions (Eldzhurtu and others, Hess et al., 1993; Chernyshev et al., 2011) within the Peredovoy Range zone. In the Late Pleistocene, magmatic activity migrated westward, in the upper reaches of the Kuban, Malka, and Baksan rivers, and produced the Elbrus neovolcanic center (less than 1 Ma). Thus, beginning from the Late Pliocene, the magmatic activity at the Greater Caucasus migrated in two directions: in the east–southeast, where Kazbek neovolcanic area was created, and northwest–west to Elbrus neovolcanic area. It is pertinent to mention that the creation of two separate practically opposite migration "vectors" of the Late Cenozoic endogenic activity occurred in the development area of the Tsana complex after cessation of magmatism in this area. In the light of the revealed spatiotemporal trends, the areal of Neogene magmatism of the Tsana Complex should be ascribed not as the western part of the Kazbek neovolcanic area (Chernyshev et al., 2006) but as the northern part of spatially close Central Georgian neovolcanic area, where volcanic activity occurred slightly earlier (7.2–6.0 Ma), and definitely represents a precursor of the intrusive magmatism in the Zemo Racha, Kvemo Svaneti, and mountainous part of North Ossetia.

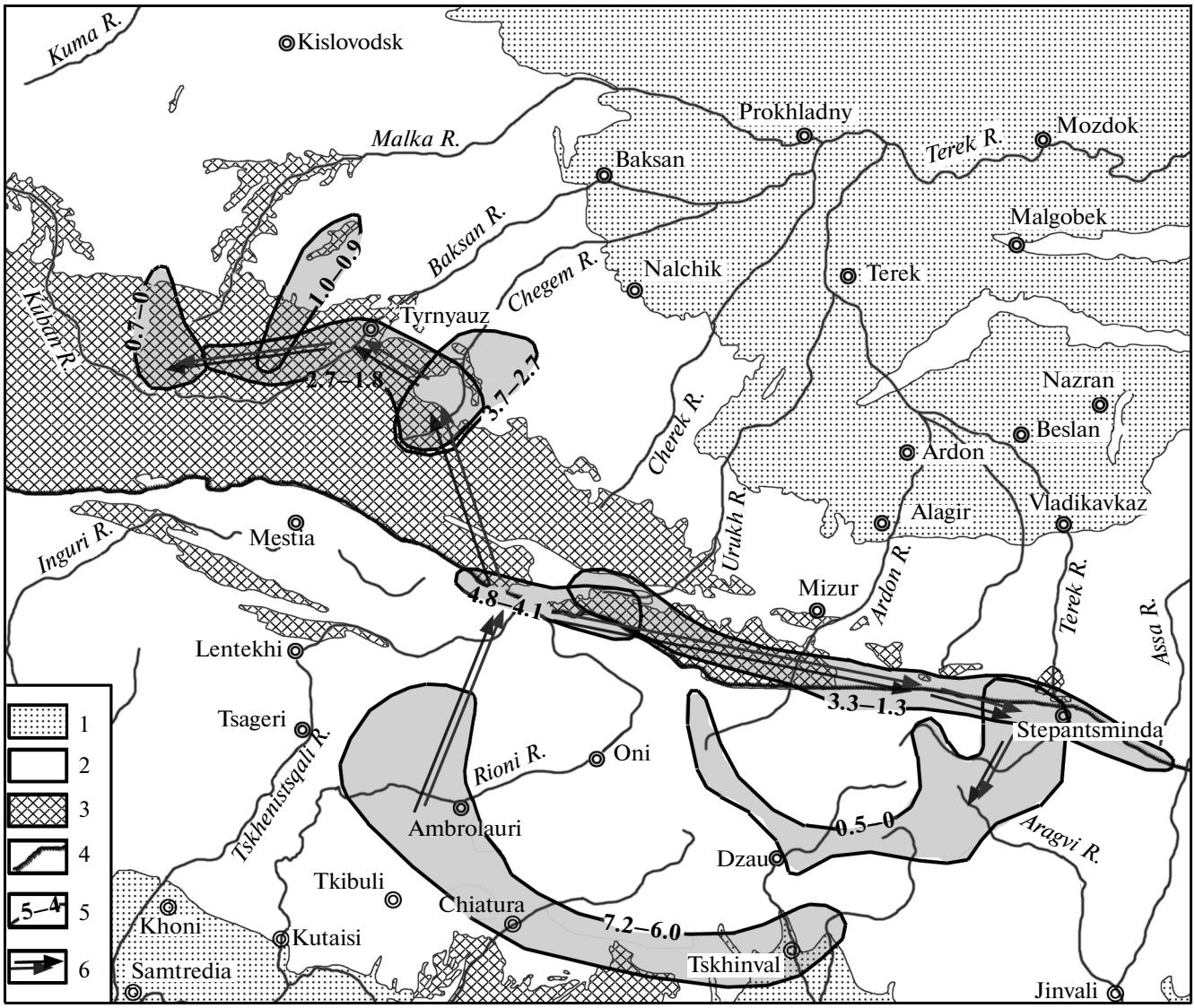

Fig. 6. Development areas of the Neogene–Quaternary magmatism of different age and its migration within the Greater Caucasus. Data are taken from (Hess et al., 1993; Gazis et al., 1995; Lebedev et al., 2006b, 2009, 2010, 2013, 2016; Lebedev and Vashakidze, 2014; Chernyshev et al., 2006; 2011). (1) Quaternary sedimentary rocks, (2) Mesocenozoic volcano-sedimentary cover, (3) exposures of the Paleozoic crystalline basement, (4) Main Caucasus Fault (upthrow fault), (5) magmatic areas (age indicated in Ma), (6) migration direction of magmatic activity.

Petrographic Characteristics of the Intrusive Rocks of the Tsana Complex

Our collection of polished thin sections characterizing the main types of the granitoids was used to describe the petrography of magmatic rocks of the Tsana Complex. Previously published data by (Kiknadze, 1967) were additionally used to characterize the petrographic features of the neointrusions of the Tsurungal group. The plutonic rocks were classified using the QAPF diagram, while subvolcanic rocks were classified using TAS diagram (Fig. 7, Le Bas et al., 1986). The main petrographic characteristics of the studied rocks are generalized in Table 3, where magmatic rocks of the Tsana Complex are grouped according to their spatial position, timing, and morphology.

The phase-I dikes and veins of the Tsurungal group of neointrusions are made up of three main rocks types: microdiorite, diroite porphyry, and granodiorite porphyry (Table 3). Two former are subdivided into quartz-bearing and quartz-free varieties. The microdiorites are usually gray or brownish holocrystalline, equigranular fine-grained rocks consisting mainly of euhedral, frequently zoned plagioclase (from sodic labradorite to oligoclase) and brown biotite flakes. Quartz occurs in variable amounts (from the complete absence to 10 vol %) as xenomorphic grains filling interstices between plagioclase crystals. Accessory minerals

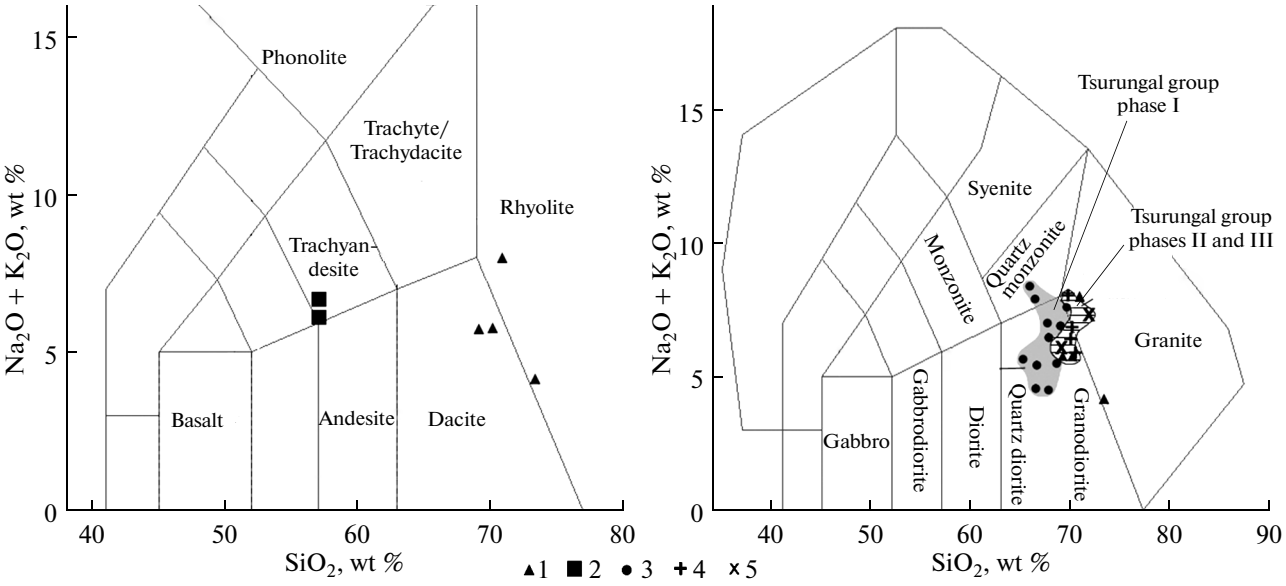

Fig. 7. SiO_2–($Na_2O + K_2O$) diagrams for the volcanic (Le Bas et al., 1986) (a) and plutonic (Middlemost, 1985) rocks (b). Karobi group: (1) rhyodacite subvolcanic bodies, (2) trachyandesite dikes. Tsurungal group: (3) diorite porphyry, quartz diorite porphyry, granodiorite, and granodiorite porphyry of phase I, (4) granite porphyry, two-mica granite, porphyritic granite of phase II, (5) leucocratic granite and aplite dikes of phase III.

are mainly represented by apatite. The diorite porphyry of dike is the dark brown porphyritic rock with phenocrysts of zoned plagioclase of variable composition (labradorite-oligoclase), biotite, and sometimes quartz (up to 4 vol %). The fine-grained, hypidiomorphic groundmass consists of oligoclase laths (sometimes unidirected) and small crystals of biotite, quartz, and very rare anorthoclase. This granodiorite porphyry differs from the diorite porphyry in the steady appearance of anorthoclase as phenocrysts and in groundmass; the amount of its phenocrysts is sometimes comparable with those of plagioclase phenocrysts. Biotite and quartz are of subordinate significance. The accessory minerals in the intermediate rocks of early dikes are dominated by apatite (up to 3 vol %), with less abundant titanite, magnetite, zircon, and rare tourmaline.

Small massifs of phase I of the Tsurungal group consist of three rock types: granodiorite porphyry, monzogranite, and diorite porphyry (Table 3). The latter may be subdivided into quartz-bearing and quartz-free varieties. The granodiorite porphyry is the light porphyritic rock with phenocrysts of zoned plagioclase (from labradorite to oligoclase), quartz, and biotite. Hypidiomorphic medium-grained groundmass is made up of the same minerals with addition of significant amount of anorthoclase (up to 20 vol %). Accessory minerals are apatite (up to 3%), zircon (up to 1%), rare magnetite, tourmaline, titanite, and cassiterite. Monzogranite is equigranular (medium-grained) rock consisting of subequal proportions of zoned plagioclase (andesine–oligoclase), anorthoclase, and quartz. The rock also contains significant amounts of biotite (up to 10 vol %) and accessory apatite (up to 1 vol %). The diorite porphyry is clearly porphyritic rock with fine grained groundmass. Phenocrysts are dominated by zoned plagioclase (from labradorite to oligoclase) at subordinate amount of biotite and quartz (0–12 vol %). Groundmass may contain up to 5 vol % *Kfs*.

The rocks of phase-II stocks of the Tsurungal group are represents by three varieties: granite porphyry, porphyritic granites, and two-mica granites (Table 3). Two former are linked by gradual transitions and differ mainly in the matrix grain size. The phenocrysts are dominated by alkali feldspar (*Ano–Mc*), which often forms antiperthitic ingrowths in plagioclase. Plagioclase and biotite occur in subordinate amounts. The pseudomorphs of secondary minerals on amphibole are very rarely observed in the rocks. Major accessory minerals are apatite and zircon. Two-mica granite is usually light equigranular medium-grained rock found only in the Chorokhi Massif. In terms of mineral composition, it differs from other types of granites in the presence of muscovite in equal amounts with biotite (6 vol % each).

The late dikes and veins of the Tsurungal group (phase III) are represented by granite porphyry, quartz porphyry, leucogranite, and aplite (Table 3). The granite and quartz porphyries are usually light rocks, with phenocrysts (up to 70 vol %) dominated by quartz and alkali feldspar (*Ano–Mc*). The rocks also contain subordinate sodic plagioclase and no more than 5–8% biotite. The quartz porphyry and aplite sometimes contain muscovite. Accessory minerals are apatite,

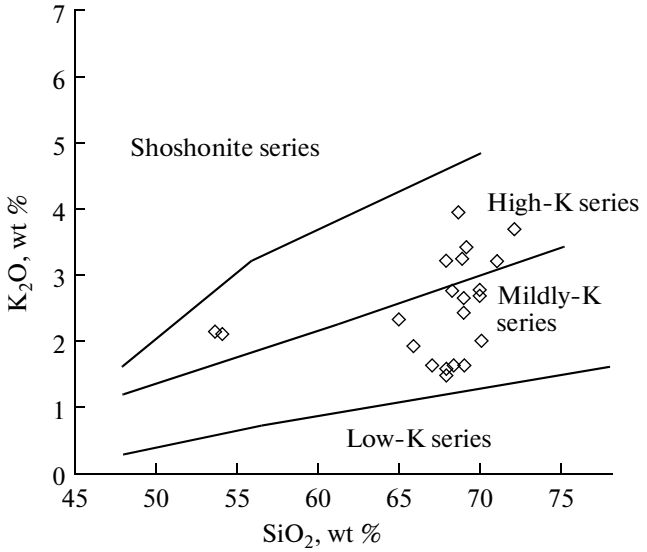

Fig. 8. SiO_2–K_2O diagram (Peccerillo, Taylor, 1976) for the studied magmatic rocks of the Tsana Complex.

zircon, tourmaline, titanite, rutile, magnetite, cassiterite, rarely andalusite and garnet.

The rhyodacite of the Karobi Group is gray porphyritic rock with phenocrysts frequently forming glomeroporphyric intergrowths (Table 3). The phenocrysts are dominated by zoned plagioclase on average corresponding to andesine. Quartz and biotite phenocrysts are observed in subordinate amounts. Microallotriomorphic groundmass is made up of the same minerals. Accessory minerals are apatite, zircon, and magnetite. The dike trachyandesite of the Karobi group is porphyritic rock with 20 vol % of phenocrysts dominated by zoned plagioclase (andesine–oligoclase), with rare quartz and amphibole. Biotite, clinopyroxene, and secondary pseudomorphs on olivine are very rare minerals. Panidiomorphic groundmass consists of plagioclase and amphibole. Accessory minerals are titanite, apatite, and magnetite.

Chemical Composition of the Intrusive Rocks of the Tsana Complex

The chemical compositions (major rock-forming oxides) of the studied magmatic rocks of the Greater Caucasus are listed in Table 4 (including author's data and data from works of Kiknadze, 1961; Togonidze and Dudauri, 2008). It is seen in the table that the intrusive and subvolcanic rocks of the Tsana complex generally show wide variations of many components.

Most mafic rocks compose the dikes in the upper reaches of the Tanadon River and correspond to trachyandesite in the SiO_2–($Na_2O + K_2O$) classification diagram for volcanic rocks (Le Bas et al., 1986) (Fig. 7). They contain 57.2–57.0 wt % SiO_2, 6.7–6.1 wt % $Na_2O + K_2O$ at 2.3–2.2 wt % K_2O (K_2O/Na_2O – 0.6–0.5), are ascribed to the K-Na mildly-alkaline series, and have high magnesium number (*mg*# 0.66–0.65). Based on the petrographic appearance, rocks from hypabyssal bodies of the Karobi ridge (Table 3) should be typified using classification for volcanic rocks. According to TAS classification (Le Bas et al., 1986), they are ascribed to rhyodacite. It should be noted that these rocks are heterogeneous in terms of content of many major oxides: they are characterized by wide variations of alkalis ($Na_2O + K_2O$—7.9–4.1 wt %), MgO (1.3–0.6 wt %) and some other components against a relatively narrow range of SiO_2 (73.4–69.2 wt %). Rhyodacite is ascribed to the calc-alkaline series (K_2O/Na_2O 0.4–0.3) and has *mg*# from 0.50 to 0.21.

The granitoids of different phases of the Tsurungal group demonstrate significant differences in the chemical composition (Table 4, Fig. 7). In the SiO_2–($Na_2O + K_2O$) diagram for plutonic rocks (Middlemost, 1985), the data points of phase I rocks fall mainly in the granodiorite—quartz diorite field and only two samples correspond to quartz monzonite (69.6–65.2 wt % SiO_2, 8.3–4.5 wt % $Na_2O + K_2O$ at 3.2–1.5 wt % K_2O, K_2O/Na_2O—0.8–0.3). They are ascribed to the calc-alkaline or much rare K-Na (or Na) mildly-alkaline (quartz monzonite) series and characterized by the wide variations of *mg*# from 0.76 to 0.32. In terms of the last parameter, the phase-I granitoids of the Tsurungal group are clearly subdivided into two subgroups: low-magnesium (*mg*# 0.47–0.32) and high-magnesium (*mg*# 0.74–0.68) rocks. Note that the range of *mg*# in the rocks of the second group is identical to that of typical granitoids of the adakite series.

The phases II and III rocks of the Tsurungal group in general are slightly more acid as compared to their earlier analogues. In the TAS diagram (Middlemost, 1985), their data points define a compact cluster at the boundary of the granite and granodiorite–quartz diorite fields (Fig. 7). The granitoids contain 71.9–69.1 wt % SiO_2, 8.0–6.0 wt % $Na_2O + K_2O$ at 4.0–2.6 wt % K_2O (K_2O/Na_2O—0.6–0.5), are ascribed to the calc-alkaline series, and have low magnesium number (*mg*# 0.43–0.09). In terms of silica and alkali relations, the late granitoids of the Tsurungal group are close to the rhyodacite of the Karobi Group and form overlapping fields in the TAS diagram (Fig. 7).

On the SiO_2–K_2O diagram (Peccerillo and Taylor, 1976), data points of the studied magmatic rocks of the Tsana Complex fall in the fields of mildly-potassium, more rarely, high-potassium rocks (Fig. 8); in the A/CNK–A/NK diagram, they define a vague trend from metaluminous to peraluminous granitoids (Fig. 9). According to the classification proposed in (Maniar and Piccoli, 1989), the petrographic characteristics, and position of data points in the A/CNK–A/NK (Fig. 9), FeO_t–MgO, and (FeO_t + MgO)–CaO diagrams (Fig. 10), these rocks may be ascribed to the

Table 4. Chemical composition (wt %) of the Pliocene intrusive rocks of the Tsana Complex (Greater Caucasus)

Sample	Rock	SiO_2	TiO_2	Al_2O_3	Fe_2O_3	FeO	MnO	MgO	CaO	Na_2O	K_2O	P_2O_5
Tsurungal group of intrusions												
Phase I												
35**	Quartz microdiorite	66.59	0.30	16.38	2.48	0.79	0.03	4.47	3.33	3.84	1.59	0.20
37**	Diorite porphyry	69.03	0.98	16.03	í.î.	2.87	0.02	1.40	2.60	4.09	2.77	0.20
127**	Granodiorite porphyry	69.60	0.31	16.52	0.73	1.77	0.02	0.79	2.47	4.30	3.24	0.24
140**	The same	67.72	0.10	16.63	1.49	0.10	0.01	2.19	4.78	3.78	3.19	0.01
332**	Diorite porphyry	67.81	0.51	15.57	1.79	2.49	0.50	1.10	3.49	4.99	1.50	0.26
338**	Granodiorite	65.24	0.57	16.46	2.66	3.71	0.06	2.11	3.41	3.31	2.31	0.15
369**	Quartz diorite porphyry	68.68	0.10	16.02	1.99	0.20	0.06	3.48	3.98	3.09	2.39	0.01
374**	Granodiorite porphyry	66.55	0.61	16.66	2.02	3.64	0.02	2.12	3.82	2.63	1.92	0.02
407**	Quartz diorite porphyry	66.43	0.60	16.33	1.61	2.52	0.01	1.31	3.10	5.95	1.92	0.21
451**	Diorite porphyry	67.80	0.40	16.35	2.39	0.30	0.02	3.99	4.21	2.90	1.56	0.09
107**	Granodiorite	65.91	0.19	16.68	1.05	1.14	0.01	2.57	3.72	5.09	3.24	0.40
Phase II												
216**	Granite porphyry	69.75	0.28	16.16	0.29	2.05	0.02	0.94	2.45	4.04	3.99	0.03
386**	Two-mica granite	70.39	0.71	18.45	0.31	2.73	0.01	0.26	1.15	2.13	3.59	0.26
397**	Porphyritic granite	70.06	0.30	15.51	1.90	3.10	0.02	0.81	1.70	3.60	2.77	0.21
461**	Granite porphyry	70.19	0.30	16.04	1.50	1.30	0.03	1.10	2.51	4.11	2.71	0.20
Phase III												
20**	Quartz porphyry	69.08	0.52	16.02	2.99	3.60	0.01	0.36	1.26	3.37	2.63	0.15
351**	The same	71.91	0.28	15.04	1.11	1.99	0.02	0.57	1.52	4.06	3.24	0.25
Karobi group of intrusions												
Dike rocks												
Ur-21	Trachyandesite	57.05	0.79	15.75	6.75	í.î.	0.12	5.87	7.23	3.87	2.20	0.36
Ur-24	The same	57.14	0.77	15.58	6.67	í.î.	0.12	5.99	6.69	4.42	2.26	0.36
Massif rocks												
R-192	Rhyodacite	69.16	0.25	15.48	1.78	2.55	0.03	0.62	4.31	4.05	1.62	0.16
R-194	The same	70.14	0.38	15.53	1.13	2.56	0.03	0.81	3.57	4.06	1.62	0.17
R-200	"	73.36	0.38	13.83	1.13	2.56	0.03	1.00	3.47	3.05	1.02	0.17
R-358*	"	70.92	0.12	14.63	0.15	2.18	0.03	1.29	2.70	5.87	2.02	0.09

Results of analyses were recalculated to 100%. n.d.—not determined. * Data from (Togonidze and Dudauri, 2008), ** data from (Kiknadze, 1961).

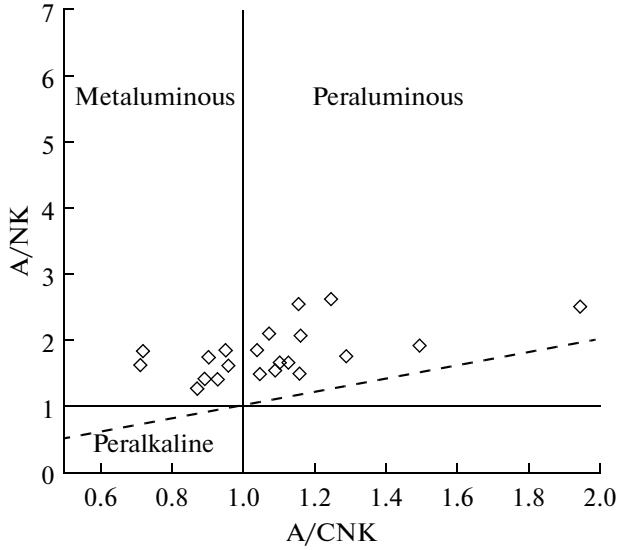

Fig. 9. Diagram A/CNK–A/NK (Maniar and Piccoli, 1989) for the studied magmatic rocks of the Tsana Complex.

postorogenic (late and post-collision) granitoids (POG) forming during later phases or immediately after cessation of continental collision.

Origin of the Granitoids of the Tsana Complex

Based on the petrographic studies of the granitoids of the Tsurungal group, Kiknadze (1967) concluded that the young rocks of the region are of hybrid origin and their magmas were formed by mixing of acid (crustal) and basic melts. This conclusion was supported by the following arguments: (1) textural and structural heterogeneity of the rocks, variable mineral composition, including alternation of the leuco- and melanocratic zones in the same parts of dikes and massifs; (2) presence of numerous variably reworked gabbroid xenoliths and microinclusions with sharp, sometimes, gradual, fused, or resorbed outlines and acid interstitial glass; (3) development of biotite rims around corroded grains of quartz and plagioclase with normal zoning, as well as "quartz eyes"; (4) inverse and oscillation zoning of many plagioclase phenocrysts; (5) frequent development of antiperthites; (6) simultaneous presence of calcic and sodic plagioclases; (7) coexistence of great amounts of quartz and *Kfs* with calcic plagioclase; (8) abundance of accessory minerals, especially apatite and more rare tourmaline; (9) simultaneous enrichment of granitoids in compatible (Ni, Co, Cr) and incompatible (Be, Zr, Ga, Sn, As, Bi) elements. Obviously, many of these facts could be considered only as indirect evidence for hybridism, but obtained new petrographic and isotope-geochemical data at least are not contradict to conclusion made by I.I. Kiknadze.

Our results show that at least three disequilibrium phenocrystic associations may be distinguished in the phases I and II porphyritic granitoids of the Tsurungal group. The first association includes normally zoned plagioclase phenocrysts with labradorite core (An 55-70) and oligoclase rim (An 25-30), which are sometimes rimmed by *Kfs* or biotite. This assemblage possibly includes rare amphibole preserved only as secondary pseudomorphs. The second association includes plagioclase phenocrysts with inverse and recurrent zoning, with albite-sodic oligoclase cores (An 10-20) and oligoclase (An 20-28) rims, and corroded quartz of the earlier generation, sometimes, with mica fringe. The

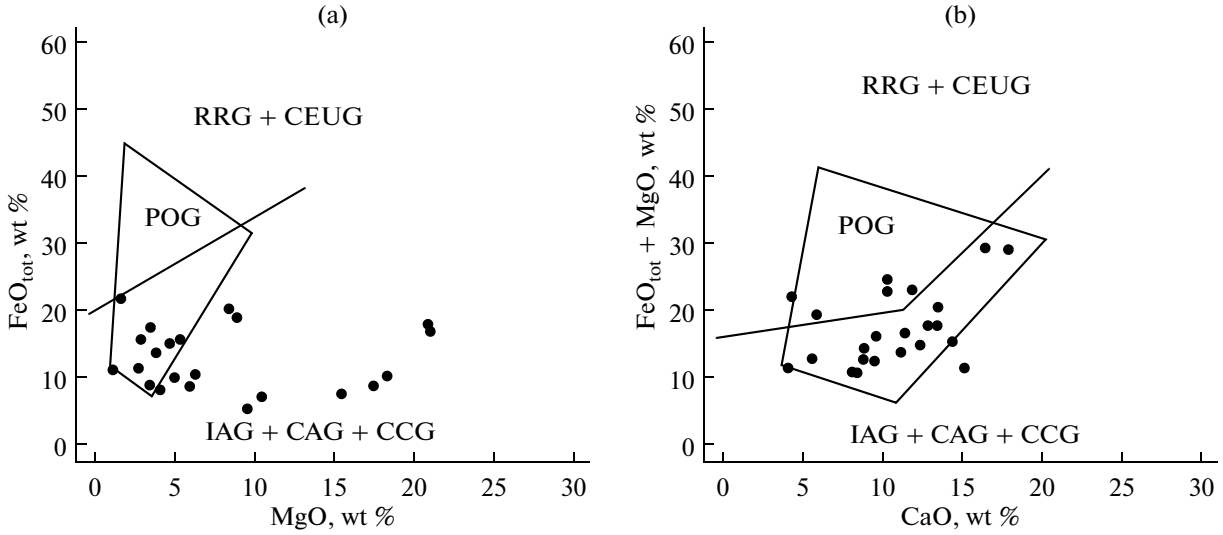

Fig. 10. Discrimination FeO_{tot}–MgO (a) and (FeO_{tot} + MgO)–CaO (b) diagrams (Maniar and Piccoli, 1989) for the studied magmatic rocks of the Tsana Complex. Granitoids: (POG) postorogenic (postcollisional), (RRG) rift-related granitoids, (CEUG) continental epeirogenic uplift granitoids (continental hot spots), (IAG) island arc granitoids, (CAG) continental arc granitoids (early collisional), (CCG) continental collisional granitoids (syncollisional).

third ("hybrid") association includes small unzoned oligoclase phenocrysts (An 21-25), as well as biotite, anorthoclase, and later quartz of groundmass. It is highly possible that the first association could be formed during crystallization of deep-seated basic-intermediate melt, while the second association crystallized in acid upper crustal melts; and the third association was formed after mixing of basic and acid magmas and formation of disequilibrium hybrid melt. Note that the disequilibrium phenocrystic associations were also found by us in the rhyodacite of the Karobi ridge (calcic plagioclase + relict amphibole, quartz + sodic plagioclase + biotite), as well as in the trachyandesite dikes of the mountainous part of North Ossetia (calcic plagioclase + olivine + clinopyroxene, quartz + sodic plagioclase + biotite, amphibole + intermediate plagioclase).

The suggested hybrid origin of the intrusive rocks of the Tsana Complex inferred from above mentioned petrographic features also agrees with some chemical peculiarities of these rocks. In particular, the studied rocks are confined to the POG field (Fig. 10) or plot in the field of I-type granites in the Na_2O–K_2O diagram (Chappell and White, 1974) (Fig. 11), which are usually regarded as granitoids of mixed mantle-crustal origin. This implies that their magmas could be product of either (1) crustal assimilation of primary mantle melts or (2) mixing of deep-seated melts with upper crustal partial melts (both versions are usually combined with crystallization differentiation).

Moreover, the hybrid origin of the granitoid magmas of the Tsana complex could be proved seriously by obtained isotope-geochemical data, in particular, obvious Sr-isotope disequilibrium between a mixture of zoned plagioclases ascribed to different mineral associations, on the one hand, and groundmass and biotite, on the other hand (Fig. 5). In addition, initial $^{87}Sr/^{86}Sr$ ratio in the studied Early Pliocene granitoids of different magmatic phases shows wide variations from 0.7053 to 0.7071 (Table 2, Fig. 5). This range sharply differs from the present-day $^{87}Sr/^{86}Sr$ ratios of the upper crustal Paleozoic granite-metamorphic rocks of the Greater Caucasus (>0.715) and the lower crust of the region (around 0.703), as well as from Sr isotope composition of basic magmas produced by asthenospheric mantle source (0.704) that was responsible for magma generation in this region in the Neogene–Quaternary (Lebedev et al., 2010). The Sr isotope composition of magmatic rocks of the Tsana complex is intermediate between mantle rocks and upper crustal complexes. In this relation, the most plausible assumption is that the parental magmas of the Tsana intrusions were derived by mixing of mantle melts with crustal melts generated by partial melting of overthickened crust that was faulted and strongly heated under upper crustal compression of the Epihercynian Skythian plate in the Main Caucasus Fault zone. It should be noted, the geophysical studies

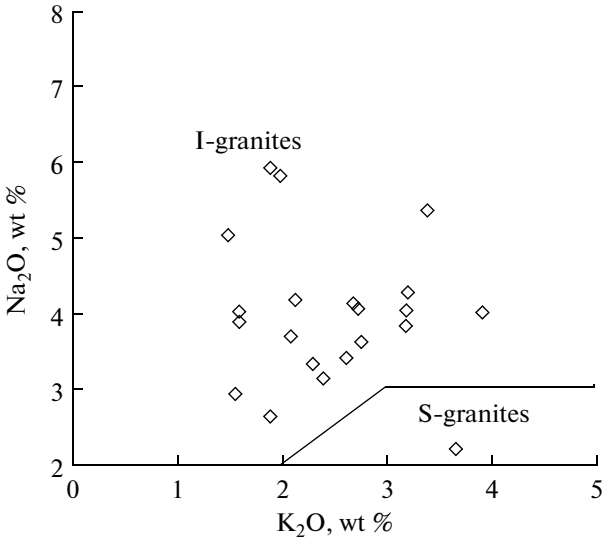

Fig. 11. Na_2O–K_2O diagram (Chappell and White, 1974) for the studied magmatic rocks of the Tsana Complex.

(Shempelev et al., 2005) suggest the presence of local melting chambers at the upper crustal levels up to the present time and the absence of sharp geophysical crust–mantle boundary in many areas in the framing of this largest regional tectonic zone.

It should be noted in conclusion that the intrusive and subvolcanic bodies of the Tsana Complex are paragenetically and may be genetically associated with complex sulfide mineralization, which forms economic, previously explored As and Mo deposits, as well as numerous Sn, Sb and Cu-base metal occurrences. At present, prospecting is in progress at the largest of these ore objects, the Tsana arsenopyrite deposit, which is regarded as promising for extraction of gold from arsenopyrite (average Au content in ores 2 ppm, Kekelia et al., 2008) from veins, wastes, and tails. Additional isotope-geochemical studies are required to establish the genetic relationships between the sulfide mineralization and Tsana neointrusions. It is important that such ore occurrences with (Au)-arsenopyrite-quartz veins were found both in the Georgian and Russian parts of the considered sector of the Greater Caucasus (for instance, the Tanadon deposit in the mountainous part of North Ossetia, Konstantinov et al., 2005), where sulfide mineralization may be also related to the evolution of the Early Pliocene magmatism.

CONCLUSIONS

(1) Young intrusive and subvolcanic bodies of the Tsana Complex were formed in the axial part of the Greater Caucasus in the neighboring regions of Georgia (Kvemo Svaneti and Zemo Racha) and Russia (mountainous part of North Ossetia) in the Early

Pliocene. They are localized within the spatially separated Tsurungal and Karobi areas. The Tsurungal group includes three stocks and dike swarm in the upper reaches of the Tskhenistsqali River. They are made up of the rocks of different composition: from diorite and granodiorite to granite porphyry and leucogranite. The Karobi group includes subvolcanic rhyodacite bodies in the upper reaches of the Chashuri River and submeridionally oriented trachyandesite dikes developed in this part of the Main Caucasus Range. All the rocks of the Tsana Complex are confined to the sublatitudinal Main Caucasus Fault spanning an area of 40 (NW–SE) × 10 (SW–NW) km in size.

(2) The results of isotope-geochronological (K-Ar, Rb-Sr) studies indicate that the igneous rocks of the Tsana Complex were formed in the Early Pliocene during two discrete pulses of magmatic activity: 4.80 ± 0.15 and 4.15 ± 0.10 Ma. The intrusive bodies of the Tsurungal Group were formed during the indicated time periods, at basic to acid evolution of magmatic melts, while the Karobi group was formed during the earlier pulse of magmatic activity.

(3) The volcanic activity at the Greater Caucasus from the terminal Pliocene to the Late Pleistocene showed a systematic spatial migration with two main displacement "vectors" of volcanic centers and related areas of intrusive magmatism (Fig. 6).

(4) Petrographic and geochemical, including isotope-geochemical, data support the hybrid nature of the young granitoid melts, with different contribution of mantle and crustal sources at different phases of the magmatic evolution of the Tsurungal and Karobi intrusive groups. Parental magmas that produced the young intrusive bodies were presumably derived by combination of fractional crystallization and mixing of deep-seated mantle magmas with upper crustal partial melts from the Epihercynian Skythian plate. The crustal contribution was minimal in the formation of the Karobi group, and played significant role in the genesis of the late-phase granitoids of the Tsurungal group. The Main Caucasus upthrow fault and subsidiary faults acted as conduits for magmas of the Pliocene granitoids of the Tsana Complex.

ACKNOWLEDGMENTS

This work was supported by the Presidium of the Russian Academy of Sciences (program no. 15) and Russian Foundation for Basic Research (project no. 14-05-00071).

REFERENCES

Belyankin, D.S., On the age problem of some Caucasian intrusions, *Izv. Geol. Kom.,* 1924, vol. 43, no. 3, pp. 409–424.

Bogina, M.M., Petrology of the Pliocene Granitoids of the Greater Caucasus, *Extended Abstract of Cand. Sci. (Geolmin) Dissertation,* Moscow: IGEM RAN, 1994.

Borsuk, A.M., *Mezozoiskie i kainozoiskie magmaticheskie formatsii Bol'shogo Kavkaza* (Mesozoic and Cenozoic Magmatic Associations of the Greater Caucasus), Moscow: Nauka, 1979.

Chappell, B.W. and White, A.J.R., Two contrasting granite types, *Pacific Geology,* 1974, vol. 8, pp. 173–174.

Chernyshev, I.V., Lebedev, V.A., and Arakelyants, M.M., K-Ar dating of Quaternary volcanics: methodology and interpretation of results, *Petrology,* 2006, vol. 14, no. 1, pp. 62–80.

Chernyshev, I.V., Lebedev, V.A., Bubnov, S.N., et al., Pliocene ignimbrites of the Elbrus area in the Neogene—Quaternary volcanism history within the Greater Caucasus (isotope–geochronological data), *Dokl. Earth Sci.,* 2011, vol. 436, no. 1, pp. 102–107.

Dokuchaev, A.Ya., Bogatikov, O.A., Gurbanov, A.G., et al., Metallogeny of Neogene granitoid magmatism of the Greater Caucasus and Cis-Caucasus: position and metallogenic evolution of the Alpine–Himalayan belt, in *Granitoidy: usloviya formirovaniya i rudonosnost'. Materialy nauchnoi konferentsii* (Granitoids: Conditions of Formation and Ore Potential: Proceedings of Conference), Kiev: Institut geokhimii, mineralogii i rudoobrazovaniya im. N.P. Semenenko, 2013, pp. 46–47.

Dubinina, E.O., Nosova, A.A., Avdeenko, A.S., and Aranovich, A.Ya., Isotopic (Sr, Nd, O) systematics of the high Sr–Ba Late Miocene granitoid intrusions from the Caucasian Mineral Waters Region, *Petrology,* 2010, vol. 18, no. 3, pp. 211–238.

Ershov, A.D., Structure of the Tsurungal (Tsena) ore field, *Probl. Sov. Geol.,* 1938, vol. 8, no. 4, pp. 270–289.

Ershov, A.D., Ore potential of the Zemo Racha and Svaneti, *Sov. Geol.,* 1940, no. 8, pp. 24–37.

Ershov, A.D. and Kopeliovich, A.V., Tsena arsenopyrite deposit of the Zemo Svaneti, *Mineral. Syr'e,* 1937, no. 2, pp. 3–13.

Gazis, C.A., Lanphere, M., Taylor, H.P., et al., $^{40}Ar/^{39}Ar$ and $^{18}O/^{16}O$ studies of the Chegem ash-flow caldera and the Eldjurta granite: cooling of two Pliocene igneous bodies in the Greater Caucasus mountains, Russia, *Earth Planet. Sci. Lett.,* 1995, vol. 134, pp. 377–391.

Hess, J.C., Lippolt, H.J., Gurbanov, A.G., and Michalski, I., The cooling history of the Late Pliocene Edzhurtinsky granite (Caucasus, Russia) and the thermochronological potential of grain-size/age relationship, *Earth Planet. Sci. Lett.,* 1993, vol. 117, nos. 3–4, pp. 393–406.

Kekelia, S.A., Kekelia, M.A., Kuloshvili, S.I., et al., Gold deposits and occurrences of the Greater Caucasus, Georgia Republic: their genesis and prospecting criteria, *Ore Geol. Rev.,* 2008, vol. 34, pp. 369–386.

Kharashvili, G.I., Ore occurrences in the upper reaches of the Chveshuri River, *Sov. Geol.,* 1940, no. 7, pp. 113–118.

Kiknadze, I.I., Petrochemical features of the young intrusive rocks of the upper reaches of the Tskhenistsqali River (Kvemo Svaneti), *Tr. Geol. Inst. AN GSSR, Ser. Miner.-Petr,* 1961, vol. 6, pp. 137–144.

Kiknadze, I.I., *Petrologiya tretichnykh intruzivnykh porod verkhov'ev r. Tskhenistskali* (Petrology of Tertiary Intrusive

Rocks of the Upper Reaches of the Tskhenistsqali River), Tbilisi: Metsniereba, 1967.

Konstantinov, M.M., Laipanov, Kh.Kh., Danil'chenko, V.A., et al., Geological structure and prospects of the Tanadon gold–arsenopyrite deposit, *Razved. Okhr. Nedr,* 2005, no. 2–3, pp. 2–10.

Koronovskii, N.V. and Demina, L.I., Late Cenozoic Magmatism of the Greater Caucasus, in *Bol'shoi Kavkaz v al'piiskuyu epokhu* (Greater Caucasus in the Alpine Epoch), Moscow: GEOS, 2007, pp. 252–284.

Le Bas, M.J., Le Maitre, R.W., Streckeisen, A., and Zanettin, B., A chemical classification of volcanic rocks based on the total alkali—silica diagram, *J. Petrol.,* 1986, vol. 27, pp. 745–750.

Lebedev, V.A., Dudauri, O.Z., and Gol'tsman, Yu.V., Early Pleistocene magmatism of the central Greater Caucasus, *Dokl. Earth Sci.,* 2016 (in press).

Lebedev, V.A., Chernyshev, I.V., Avdeenko, A.S., et al., Heterogeneity of Ar and Sr initial isotopic composition in the coexisting minerals from Miocene hypabyssal granitoids in the Caucasian Mineral Waters region, *Dokl. Earth Sci.,* 2006a, vol. 410, no. 1, pp. 1070–1074.

Lebedev, V.A., Chernyshev, I.V., Chugaev, A.V., et al., K-Ar Age and Sr-Nd characteristics of subalkali basalts in the central Georgian Neovolcanic Area (Greater Caucasus), *Dokl. Earth Sci.,* 2006b, vol. 408, no. 4, pp. 657–661.

Lebedev, V.A., Bubnov, S.N., Chernyshev, I.V., et al., Geochronology and genesis of the young (Pliocene) granitoids of the Greater Caucasus: Dzhimara multiphase massif of the Kazbek neovolcanic area, *Geochem. Int.,* 2009, vol. 47, no. 6, pp. 550–567.

Lebedev, V.A., Chernyshev, I.V., Chugaev, A.V., et al., Geochronology of eruptions and parental magma sources of Elbrus Volcano, the Greater Caucasus: K-Ar and Sr-Nd-Pb isotope data, *Geochem. Int.,* 2010, vol. 48, no. 1, pp. 41–67.

Lebedev, V.A., Chernyshev, I.V., Dudauri, O.Z., et al., Manifestations of Miocene acid intrusive magmatism on the southern slope of the Greater Caucasus: first evidence from isotope geochronology, *Dokl. Earth Sci.,* 2013, vol. 450, no. 3, pp. 550–555.

Lebedev, V.A. and Vashakidze, G.T., The catalogue of Quaternary volcanoes of the Greater Caucasus based on geochronological, volcanological and isotope-geochemical data, *J. Volcanol. Seismol.,* 2014, vol. 8, no. 2, pp. 93–107.

Maniar, P.D. and Piccoli, P.M., Tectonic discrimination of granitoids, *Geol. Soc. Am. Bull.,* 1989, vol. 101, pp. 635–643.

Middlemost, E.A.K., *Magmas and Magmatic Rocks. An Introduction to Igneous Petrology,* London–New York: Longman, 1985.

Pecerillo, A. and Taylor, S.R., Geochemistry of Eocene calc-alkaline volcanic rocks from Kastamonu area, northern Turkey, *Contrib. Mineral. Petrol.,* 1976, vol. 58, pp. 63–81.

Pohl, I.R., Hess, Yu.S., Kober, B., et al., Origin and genesis of the Miocene trachyrhyolites (A-type) from the northern Greater Caucasus, in *Magmatizm riftov i skladchatykh oblastei* (Magmatism of Rifts and Folded Areas), Moscow: Nauka, 1993, pp. 108–125.

Shempelev, A.G., Prutskii, N.I., Kukhmazov, S.U., et al., Materials of geophysical studies along the near-Elbrus profile (Elbrus volcano–Caucasian Mineral Waters), in *Tektonika zemnoi kory i mantii. Tektonicheskie zakonomernosti razmeshcheniya poleznykh iskopaemykh: Materialy 38 Tektonicheskogo soveshchaniya* (Tectonics of the Earth's Crust and Mantle. Tectonic Control of the Distribution of Mineral Resources. Proceedings of the 38th Tectonic Conference), Moscow: GIN RAN, 2005, vol. 2, pp. 361–365.

Sobolev, R.N. and Kononov, O.V., New data on the stages of the formation of the Eldzhurtu granite massif, North Caucasus, *Dokl. Akad. Nauk,* 1993, vol. 330, no. 3, pp. 360–362.

Steiger, R.H. and Jager, E., Subcomission on geochronology: convention on the use of decay constants in geo- and cosmochronology, *Earth Planet. Sci. Lett.,* 1977, no. 36, pp. 359–362.

Togonidze, M.G. and Dudauri, O.Z., Pliocene volcanic center on the southern slope of the Greater Caucasus within the limits of Upper Racha, *Tr. Inst. Geol. Gruzii, Novaya Ser.,* 2008, no. 124, pp. 232–237.

Translated by M. Bogina